# THERMOPHYSICAL PROPERTIES OF W - RE ALLOYS ABOVE THE MELTING REGION <sup>1</sup>

# V. Didoukh<sup>2</sup>, A. Seifter<sup>3</sup>, G. Pottlacher<sup>3, 4</sup> and H. Jäger<sup>3</sup>

In earlier experiments we have studied pure elements with a fast pulse heating technique to obtain thermophysical properties of the liquid state. We report here results of thermophysical properties such as specific heat and dependencies between enthalpy, electrical resistivity and temperature, for four W - Re alloys (3.95, 21.03, 23.84 and 30.82 at % of Re) in a wide temperature range covering solid and liquid state. Thermal conductivity is calculated using the WIEDEMAN-FRANZ-law for the liquid alloy, as well as data for thermal diffusivity for the beginning of the liquid phase. Additionally, data for the entire temperature range studied have been analysed in comparison with those of the constituent elements Tungsten and Rhenium, since the both metals have been previously studied with the same experimental technique. Such information is of interest in the field of metallurgy since the W-Re alloys of small Re-content in the region of mutual component solubility in solid state are widely used as thermoelectrode materials for the purposes of high-temperature thermometry.

KEY WORDS: electrical resistivity; enthalpy; high temperature; liquid alloys; rhenium-alloy; specific heat; thermal conductivity; thermal diffusivity; tungsten - alloy.

 $^{1}\mbox{Paper}$  submitted to the  $13^{\mbox{th}}$  Symposium on Thermophysical Properties in Boulder, CO USA, June 22 - 27.1997

<sup>2</sup>Institute of Applied Physics, Ivan Franko State University, Pushkin Street 49, 290044, Lviv, Ukraine

<sup>3</sup>Institut für Experimentalphysik, Technische Universität Graz, Petersgasse 16, A - 8010 Graz, Austria

<sup>4</sup>To whom correspondence should be addressed.

#### 1. INTRODUCTION.

High temperature experimentation with solid and especially liquid substances faces a lot of difficulties. Advanced stationary steady-state measuring techniques are limited to temperatures of about 2300 K. Therefore, they can not be applied for investigations of thermophysical properties of highly melting elements, for instance refractory metals. The latter in turn are widely used as constructive materials of the static high-temperature experimental equipment.

Fast dynamic pulse-heating methods have been developed to extend the measurements to extremely high temperatures by heating up the specimen in a very short time into liquid state while the sample keeps its initial geometrical shape because of inertia [1, 2]. Since most metals and their alloys can be produced in wire-shaped form of appropriate dimensions, pulse heating techniques are found to be measuring methods of general importance for the investigation of thermophysical properties of electrically-conducting solids and fluids. This way pure refractory metals, even the highest melting ones like tungsten and rhenium, have been intensively studied during last decades [3 - 10] and the properties for almost all these metals in solid and liquid states were determined with rather good precision. However, alloys of the refractory metals, despite the prospects of their practical application, still remain less investigated up to now. Practically, there are no systematic data about thermophysical properties of these alloys in the liquid state. In best cases the information is available only for the solid state [11 - 14].

Tungsten and rhenium have the highest melting temperatures among the metals, i. e. 3695 K and 3453 K respectively. The phase diagram of the binary W-Re alloys system presented in handbook edition [15] is based mainly on the results of [16], except for the solidus of the terminal phases, which are taken from [17]. In solid state the solubility of Re in W is equal 37 at.% at 3273 K accordingly to [16] or even up to 45 at% at 3163 K as reported in [17].

To the best of our knowledge we report here the first time properties of solid and especially of liquid W-Re alloys in the concentration range of continuous solid Re in W solutions. The

information is of interest in the field of refractory metals metallurgy, since such alloys are widely used as thermoelectrode materials for the purposes of high temperature thermometry.

#### 2. EXPERIMENTAL.

Wire shaped W-Re alloys specimens with a typical length of 50 mm and 0.35 or 0.5 mm in diameter are resistively volume heated into the liquid phase by passing a large current pulse through them. Heating rates of about  $10^8$  K·s<sup>-1</sup> were achieved. The measurements were performed in air at atmospheric pressure.

The discharge circuit consists of a capacitor bank (500  $\mu$ F), a fast acting main switch and an experiment chamber. A crowbar switch allows to stop the experiment at any prechosen time. For optical diagnostics, a single wavelength pyrometer (850 nm, 10 nm bandwidth) [18] and a fast acting CCD-array, combined with a multi-chanellplate [19] were used.

Time-resolved (with sub- $\mu$ s resolution) quantities being simultaneously measured in one experiment are the current through the specimen, the voltage drop along the specimen and the surface radiation intensity. The volume expansion of the wire is recorded with a framing CCD-camera, which takes pictures of the diameter of a small part of the specimen every  $10~\mu$ s. These pictures are processed by means of an image converting system. They indicate the stability of the specimen during the time of the experiment (about  $80~\mu$ s).

The measured data are recorded by fast digital oscilloscopes, which are placed in a shielded room, and processed after the experiment. In this way, data for enthalpy, temperature, and electrical resistivity as function of time are obtained. By elimination of the quantity time one gets temperature dependencies of the above mentioned properties. For pure metals all evaluations are usually based on the assumption that the normal spectral emissivity  $\epsilon(\lambda,T)$  has the same always has the same value for the liquid metal as at melting temperature  $(T_{ref})$  and the ratio of emissivities in Eq.(1) is 1. Temperatures are calculated forming ratios of the radiance at temperature  $T_{ref}\{J_{ref}(T_{ref})\}$  given by (1). The reference temperature  $T_{ref}$  is taken from literature data [15]:

$$T = \frac{c_2}{\lambda \ln\left\{1 + \frac{J_{ref}(T_{ref})\varepsilon(\lambda, T)}{J(T)\varepsilon(\lambda, T_{ref})}\left[exp\left(\frac{c_2}{\lambda T_{ref}}\right) - 1\right]\right\}}$$
 (1)

Here J is the radiance intensity, T the temperature,  $\lambda$  the wavelength,  $\varepsilon$  the normal spectral emissivity of the specimen surface,  $c_2$  is the second radiation constants.

Fast pulse heating experiments, that reach into the liquid phase generally have to handle this problem of unknown emissivity of the liquid metal [3, 4, 5]. Recent measurements on the emissivity of liquid metals [20] will improve the accuracy of temperature measurements with fast pulse heating techniques.

In contrast to pure metals, alloys have a certain melting region instead of the melting temperature. The absence of a clearly detectable melting point, as well as possible variation of the surface radiation intensity within the melting region complicate the proper choice of a reference temperature. Therefore, in the present work for each of the investigated alloys an averaged value of respective solidus and liquidus temperatures from the phase diagram was adopted as reference melting temperature for the experimental data processing. These values together with other parameters, such as density, chemical composition, and diameter of the wire samples are given in Tab. 1 for each alloy studied.

Table 1. Parameter of wire samples, \* calculated values assuming that each component contributes to the sample density in proportion to its percent weight in the alloy.

Sample,	Conc. at.% of Re	Weight % of Re	Density*, g/cm <sup>3</sup>	T <sub>ref.</sub> ,	Diameter,
1	3,95	4.00	19.3627	3618	0.35
2	21,03	21.24	19.6377	3423	0.35
3	23,84	24.07	19.6835	3398	0.35
4	30,82	31.09	19.7983	3358	0.50
W			19.30	3683	
Re			21.0	3180	

Thermal conductivity  $\lambda$  may be evaluated from electrical resistivity by the Wiedemann-Franz law which relates electrical and thermal conductivites:

$$\lambda = L \cdot T \cdot (1/\rho), \tag{2}$$

where L is the Lorenz number  $(2.45 \times 10^{-8} \text{ V}^2 \cdot \text{K}^{-2})$ , T is temperature and  $\rho$  is the electrical resistivity of the specimen. As discussed in [21] the principal carriers for the thermal conduction in solid metals are electrons and lattice waves. However for temperatures close to the melting point of pure metals, electronic conduction is the predominant mechanism and lattice conduction is negligible. Also the Lorenz number L for most pure metals is close to its theoretical value. This way Eq. (2) is a good tool to obtain thermal conductivity in the vicinity of the melting point.

Furthermore, it is also possible to evaluate thermal diffusivity a, which is related with thermal conductivity  $\lambda$ , specific heat  $c_p$  and density d of the material

$$a = \lambda \cdot (c_p \cdot d). \tag{3}$$

For more details on measuring procedure and experimental data processing see [22].

## 3. RESULTS

As already mentioned, alloys in contrast to pure metals have the melting region instead of a clearly detectable melting point. Therefore, special attention was devoted to a proper choice of the reference temperature, because W-Re system alloys expose a rather wide temperature interval of melting in the investigated range of concentrations [15]. Fig.1 illustrates temperature dependencies of enthalpy measured in one single experiment for the sample N4, but processed for three different values of the reference temperature  $T_{ref.}$ , namely  $H_1$  for  $T_{sol.}$ ,  $H_3$  for  $T_{liq.}$ , and  $H_2$  for  $T_{ref.} = (T_{sol.} + T_{liq.})/2$ , where  $T_{sol.}$  and  $T_{liq.}$  were taken from the phase diagram [15].

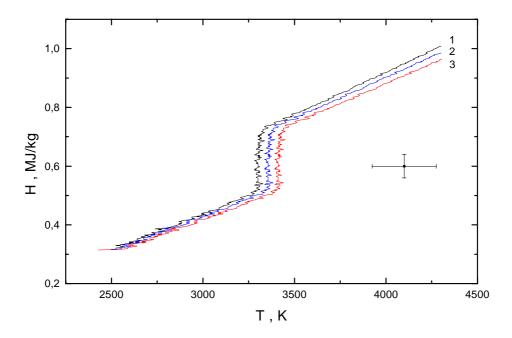


Fig.1: Illustrates temperature dependencies of enthalpy measured in one single experiment for the sample N4, but processed for three different values of the reference temperature (1:  $T_{sol.}$ , 2:  $(T_{sol.} + T_{liq.})/2$ , and 3: $T_{liq.}$ )

The heat of fusion, being obtained from the difference between the value of absorbed energy at the end of the melting region and the absorbed energy at the beginning of the melting plateau, seems to be insensitive to a variation of the reference temperature between  $T_{sol.}$  and  $T_{liq.}$ . The enthalpy in liquid and solid states increases linearly with temperature. This dependency may be described by a linear least-squares fit and its slope yields a specific heat value. Because of the lack of sharp discontinuities at the beginning and at the end of the melting region, those data points, which lie in the transition between premelting and the plateau and postmelting and the plateau were excluded from the data fits.

This way we have obtained in Fig. 1 for the same material the following three values 292.2, 280.4, and 270.4  $J \cdot kg^{-1} \cdot K^{-1}$  of the specific heat in the liquid for the three reference temperatures  $T_{sol.}$ ,  $(T_{sol.} + T_{liq.})/2$ , and  $T_{liq.}$ . The difference between maximal and minimal values does not exceed 8%. Up to 15 % uncertainty of specific heat values in pulse heating experiments have to be assumed, therefore, temperatures averaged between respective solidus

and liquidus points of each alloy concentration were taken as reference for the processing of experimentally measured data. These temperatures are also listed in Table 1.

Fig. 2 presents enthalpy as a function of temperature for the sample 4. The full lines represent least-squares fits to the data averaged over 10 best individual experiments, while the open circles show the original data of a typical single measurement. During the melting transition enthalpy changes from  $H_s = 0.516$  MJ·kg<sup>-1</sup> to  $H_l = 0.734$  MJ·kg<sup>-1</sup>, yielding  $\Delta H = 0.218$  MJ·kg<sup>-1</sup> for the latent heat of fusion.

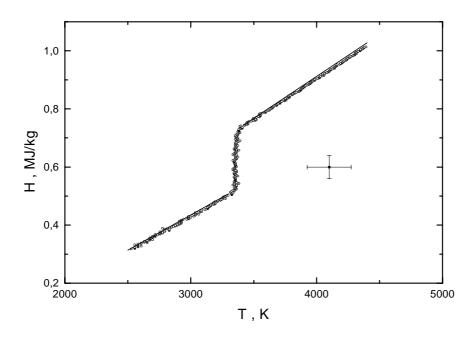


Fig. 2: Enthalpy as a function of temperature for sample 4. Full lines: least-squares fits to the data averaged over 10 best individual experiments, open circles: original data of a typical single measurement.

The dependence of enthalpy on temperature for solid and liquid states is described by the following expressions, where H is in MJ·kg<sup>-1</sup> and T in K:

$$H = -0.29388 + 0.2429 \cdot 10^{-3} T$$
 in the range  $2500 < T < 3300$  (4)

and

$$H = -0.24507 + 0.2893 \cdot 10^{-3} T$$
 in the range  $3430 < T < 4400$  (5)

The derivative of the above linear regressions gives  $c_p = 2423 \text{ J} \cdot \text{kg}^{-1} \cdot \text{K}^{-1}$  and  $c_p = 289 \text{ J} \cdot \text{kg}^{-1} \cdot \text{K}^{-1}$  for the specific heat of the alloy N4 in solid and liquid states respectively. The least-squares fits which summarise measured H(T) dependencies for the other alloys investigated in this work are given below and illustrated in Fig. 3:

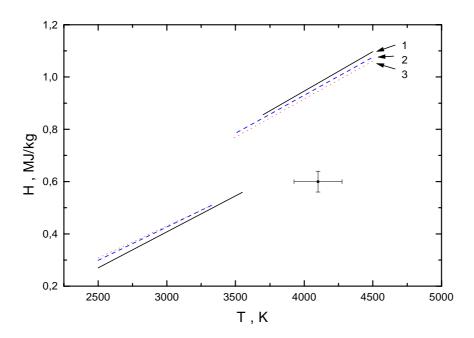


Fig. 3: Enthalpy as a function of temperature for samples N1, N2, N3 in form of least squares fits.

Alloy N3	$H = -0.30285 + 0.2443 \cdot 10^{-3} T$	in the range $2500 < T < 3300$	(6)
and	$H = -0.24523 + 0.2902 \cdot 10^{-3} T$	in the range 3490 < T < 4400	(7)
Alloy N2	$H = -0.34065 + 0.2556 \cdot 10^{-3} T$	in the range 2500 < T < 3340	(8)
and	$H = -0.23415 + 0.2911 \cdot 10^{-3} T$	in the range 3510 < T < 4400	(9)
Alloy N1	$H = -0.41911 + 0.2756 \cdot 10^{-3} T$	in the range 2900 < T < 3550	(10)
and	$H = -0.26164 + 0.3020 \cdot 10^{-3} \text{ T}$	in the range 3700 < T < 4500	(11)

The electrical resistivity for each of the alloys was determined from the same experiments that were used to calculate enthalpy and specific heat. Fig. 4 presents the electrical resistivity of alloy N3 ( $\rho_0$  - not corrected and  $\rho$  - corrected for thermal expansion) as a function of temperature in form of least-squares fits. The results of a single typical measurement are given again as open circles.

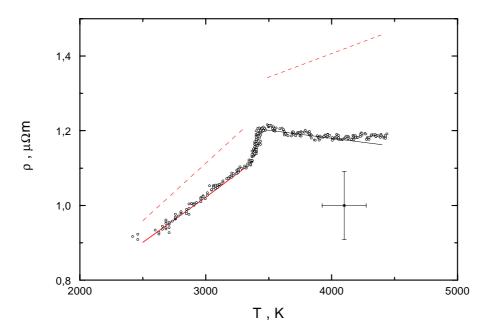


Fig. 4: Electrical resistivity of alloy N3 (least-squares fit for  $\rho$  (corrected for thermal expansion) as dashed line, and least-squares fit  $\rho_0$  (not corrected as a full line) as a function of temperature. Open circles: results of a single measurement.

The determined dependencies may be described by the following two expressions for uncorrected resistivity  $\rho_0$ , in  $\mu\Omega m$ , T in K:

$$\rho_0 = 2.9045 + 2.44 \cdot 10^{-3} \cdot T$$
 in the range 2500

$$\rho_0 = 1.351194 \cdot 10^1 - 4.28743 \cdot 10^{-4} \cdot T$$
 in the range 3490

and for volume corrected resistivity  $\rho$  in  $\mu\Omega$ m, T in K:

$$\rho = 1.8963 + 3.07733 \cdot 10^{-3} \cdot T$$
 in the range 2500

$$\rho = 8.999 + 1.26691*10^{-3} \cdot T$$
 in the range 3490

for solid and liquid states respectively.

The other W-Re alloys investigated in this work expose a very similar temperature behaviour of non-corrected resistivity, i. e. increasing in the solid state and decreasing for the liquid state. By means of least-squares fits, the following functional  $\rho_0(T)$  dependencies were obtained from a large number of experimental data points:

Alloy N1 
$$\rho_0 = 1.79186 + 2.57 \cdot 10^{-3} \text{T}$$
 for the range 2900

and 
$$\rho_0 = 1.298049 \cdot 10^1 - 2.15784 \cdot 10^{-4} \cdot T$$
 for the range 3700

Alloy 2. 
$$\rho_0 = 2.94835 + 2.48 \cdot 10^{-3} \text{T}$$
 for the range 2500\rho\_0 = 1.439627 \cdot 10^1 - 5.82841 \cdot 10^{-4} \cdot \text{T} for the range 3510\rho\_0 = 2.56844 + 2.65 \cdot 10^{-3} \text{T} for the range 2500\rho\_0 = 1.410894 \cdot 10^1 - 5.0112 \cdot 10^{-4} \cdot \text{T} for the range 3430

In Fig.5 the plots of Eq.(16 - 21) are given.

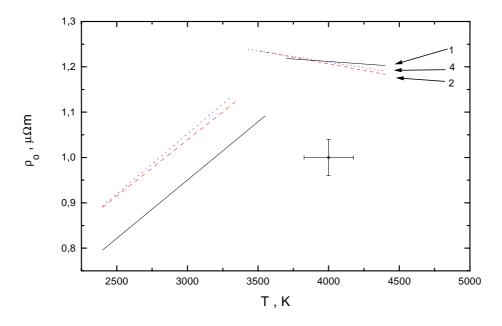


Fig. 5: Electrical resistivity  $\rho_0$  (not corrected) of alloys N1, N2, N4, as a function of temperature in form of least squares fits.

The set of experimentally determined properties allows to calculate from Eq. (2, 3) temperature behaviour of thermal conductivity  $\lambda$  and thermal diffusivity a. As an example, Fig. 6 shows the results of such an estimation for alloy N3.

The absolute values of these properties and their dependencies on temperature are described ( $\lambda$  is in W/Km, and a in  $100\text{cm}^2/\text{s}$ ) by:

$$\lambda = 5.38725 + 3.9995 \cdot 10^{-4} \cdot T$$
 in the range 2500

$$\lambda = 2.43702 + 0.00113 \cdot 10^{-4} \cdot T$$
 in the range 3490

$$a = 1.04124 + 1.49329 \cdot 10^{-4} \cdot T$$
 in the range 2500

$$a = -0.20218 + 4.1489 \cdot 10^{-4} \cdot T$$
 in the range 3490

for solid and liquid states respectively.

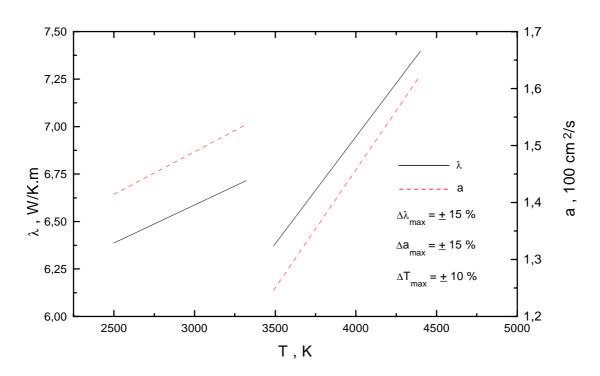


Fig. 6: Thermal conductivity  $\lambda$  (full line) and thermal diffusivity a (dashed line) as a function of temperature for alloy N3.

The values of specific heat of the W-Re alloys in solid and liquid states, their melting enthalpies, enthalpies and uncorrected resistivity values at the beginning and at the end of melting, compared with results on pure tungsten and rhenium, are summarised in Table 2.

# 4. ESTIMATE OF UNCERTAINTIES

Enthalpy is the most accurate of all the properties measured, with an estimated uncertainty of  $\pm 4$  %. For temperature measurements the uncertainty is  $\pm 5$  % in the melting region, increasing to about  $\pm 10$  % in the liquid phase. The error in the uncorrected electrical resistivity is estimated to be  $\pm 4$  %, increasing to  $\pm 7$  % for the corrected electrical resistivity. An error of  $\pm 5$  % is estimated for the density in the solid phase, increasing for the highest values in the liquid phase up to  $\pm 10$  %. The estimated uncertainty in the value of melting enthalpy is  $\pm 5$  %, the estimated uncertainty of specific heat should not exceed  $\pm 15$  %, of thermal conductivity and thermal diffusivity  $\pm 15$  %. The individual error bars are indicated in each figure.

Table 2: Values of specific heat of the W-Re alloys in solid and liquid states, melting enthalpies, enthalpies and uncorrected resistivity values at the beginning and at the end of melting, compared with literature data of tungsten and rhenium.

Sample	Ref.	H <sub>s</sub> MJ/kg	H <sub>l</sub> MJ/kg	ΔH MJ/kg	$ ho_{ m s}$ μ $ m \Omega m$	ρ <sub>l</sub> μΩm	$c_{p \text{ (sol)}}$ $\mu\Omega m$	c <sub>p (liq)</sub> J/kg•K	c <sub>p (calc)</sub> J/kg•K
		U			•		•		Ū
Alloy 4	this work	0.516	0.734	0.218	$1.14(\rho_0)$	$1.24(\rho_0)$	243	289	288.
Alloy 3	this work	0.524	0.750	0.226	$1.12(\rho_0)$	$1.23(\rho_0)$	244	290	292
Alloy 2	this work	0.529	0.763	0.234	$1.15(\rho_0)$	$1.24(\rho_0)$	256	291	293
Alloy 1	this work	0.568	0.827	0.259	$1.11(\rho_0)$	$1.23(\rho_0)$	270	302	303
Re	[4]	0.520	0.670	0.150	1.20(ρ)	1.37(ρ)		250	
	[3]	0.615	0.768	0.153	1.451(ρ)	1.457(ρ)	226	267	
	[10]							225	
	[5]	0.577	0.735	0.158	1.180(ρ)	1.188(ρ)	180	233	
W	[6]	0.629	0.885	0.256	1.179(ρ)	1.38(ρ)		305	
	[9]	0.617	0.881	0.264	1.20(ρ)	1.35(ρ)		310	
	[8]	0.61	0.87	0.26	1.26(ρ)	1.46(ρ)		262	
	[7]	0.616	0.87	0.254	1.23(ρ)	1.38(ρ)		300	

### 5. DISCUSSION

As can be seen from the data collected in Table 2, the investigated W-Re alloys have enthalpy values at the beginning and the end of melting, comparable with those of pure W and Re (see Fig. 7). Furthermore, for each alloy the enthalpy at the end of melting does not exceed the respective value of pure tungsten and decreases continuously with increasing of Re contamination, as it could be expected. The enthalpy at the beginning of melting shows the same concentration dependency, but the absolute values are lower as those reported for rhenium in [3, 5], and are very close (with exception of the alloy N1) to the  $H_s$  value reported in [4]. However, even in this case the enthalpy at the beginning of melting of the alloy with highest Re content (sample 4,  $H_s$ =0,516 MJ/kg) is a little bit lower than the lowest value of 0,520 MJ/kg reported for pure rhenium [4]. Since enthalpy is a linear function of temperature, the  $H_s$  dependency on the component concentration reflects a shape of the solidus line on the

phase diagram. In other words, our minimal  $H_s$  value for sample 4 evidently shows, that its solidus temperature is lower than the melting point of pure rhenium, and Fig. 7 may be considered as a part of the W-Re phase diagram in the enthalpy-concentration plane.

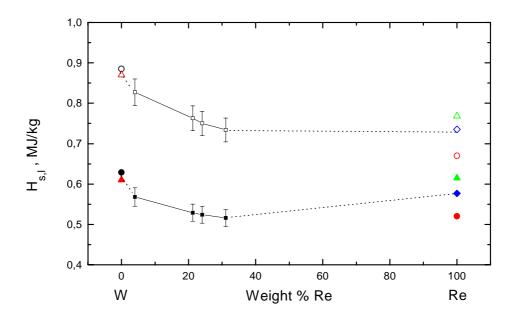


Fig. 7: Enthalpy values at the beginning (small full squares) and the end of melting (small open squares) for different weight % Re, compared to those of pure W and Re. Full figures indicate begin and empty figures indicate end of melting. Triangles: Hixson and Winkler for Re [3] and Hixson and Winkler for W [8] Circles: Kaschnitz et al. for W [6] and Pottlacher et al. for Re [4]. Squares on top: Thevenin for Re [5].

To our opinion, such diagrams give important additional information for purposes of metallurgy, especially for highly melting alloys in the region of their solid-liquid transition. Moreover, in the case of W-Re alloys the solidus and liquidus curves were not exactly measured, but rather suggested. We have found no information about exact melting temperatures for W-Re alloys containing less than 38 wt.% Re in both original publications [16, 17]. To the best of our knowledge, the solidus temperature was exactly measured only for one W-Re alloy with 3.24 wt.% Re by means of a fast dynamic technique [11]. The value reported (3645K) is higher than the reference temperature adopted in our evaluation for alloy of 4 wt% Re (see Table 1). This fact, namely the absence of exactly determined solidus and

liquidus temperatures and therefore an increased uncertainty in the choice of the reference temperature, should be always taken into account while considering and discussing all the expressions given above. However, even under this circumstance, the uncorrected resistivity for all W-Re alloys in the liquid state is a decreasing function of the temperature. This may be caused by an influence of rhenium which demonstrates the same behaviour [4, 5]. Nevertheless, volume-corrected resistivity shows a temperature dependency typical for metals (see Fig.4) with slightly increasing resistivity with temperature at the beginning of the liquid phase. It should be pointed out, that volume measurements are difficult to make in a fast dynamic experiments. In our case it was extremely difficult due to strong light radiation of the wires in the liquid state approaching the intensity of the back-ground flash used. Since volume is needed to calculate resistivity and consequently thermal conductivity as well as diffusivity, this uncertainty is reflected in these data for sample N3 as well.

To the best of our knowledge the measurements of the heat of fusion for the W-Re alloys as well as their heat capacities in the liquid state have never been performed before. Consequently, there are no data for comparison to our results. However, following the procedure used in [23], an estimated value for each single alloy can be computed from values of the heat of fusion of the constituent metals in the alloy, assuming that each metal contributes to the total heat of fusion in proportion to its percent weight in the alloy. The computations were performed using the values for heat of fusion of tungsten and rhenium being previously measured with the same experimental technique to be equal 0.256 MJ/kg [6] and 0.150 MJ/kg [4] respectively. The computed values are equal 251.7; 233.5; 230.5; and 223 MJ/kg for the alloys N1, N2, N3, and N4 respectively. As can be seen, the experimentally determined values are in quite good agreement with these estimates.

The same relationship for specific heat of alloys in the liquid state is well known as Kopp's law [24]. The calculations were performed based on the  $c_p$  values for liquid tungsten and rhenium obtained previously using the same pulse-heating technique [4, 6]. As can be seen from Table 2 and in Fig. 8, the calculated  $c_p$  values for all investigated W-Re alloys almost coincide within experimental error limits with those derived numerically from the H(T) diagrams. Since these experiments were performed for alloys in the concentration range of

solid solutions [15], it can be suggested that this rule also might be valid for other highly-melting binary alloys for respective regions of their phase diagrams. Systematic investigations of the Ni - Fe system with this fast pulse heating technique [25] demonstrate the same behaviour.

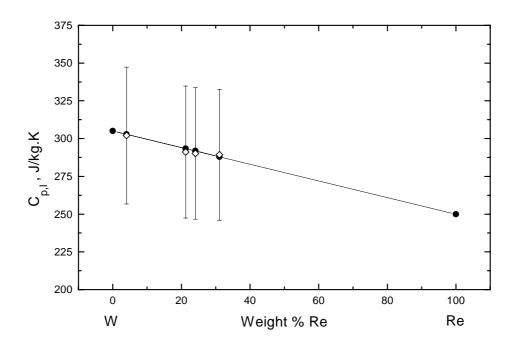


Fig. 8: Calculated  $c_p$  values for all investigated (full circles) and experimental obtained values (open squares).

# 6. ACKNOWLEDGEMENTS

One of us (V. D.) would like to thank the Technical University Graz for a research fellowship. We also thank Dipl.-Ing. Dr. P. Golob from the Forschungsinstitut für Elektronenmikroskopie und Feinstrukturforschung, Steyrergasse 17/III, 8010 Graz for determination of samples composition by means of EDAX.

### **REFERENCES**

- A. Cezairliyan, Compendium of thermophysical Property Measurements Methods, Vol.1, Ch. 16, K. D. Maglic, A. Cezairliyan and V. E. Peletsky Editors, Plenum Press, New York, (1984).
- 2.G. Pottlacher, in Advances in Materials Science and Engineering, third Supplement, R. W. Cahn Editor, Pergamon Press, Oxford, pp 2056 (1993).

- 3. R. S. Hixson, M. A. Winkler, Int. J. Thermophys. 13: 477 (1992).
- 4. G. Pottlacher, T. Neger, H. Jäger, Int. J. Thermophys. 7:149 (1986).
- 5. Th. Thevenin, L. Arles, M. Boivineau, J. M. Vermeulen, Int. J. Thermophys. 14:441 (1993).
- 6. E. Kaschnitz, G. Pottlacher, L. Windholz, *High Pressure Research*. **4**:558 (1990).
- 7. A. Berthault, L. Arles, J. Matricon, *Int. J. Thermophys.* **7**(1):167 (1986).
- 8. R. S. Hixson, M. A. Winkler, Int. J. Thermophys. 11(4):709 (1990).
- 9. U. Seydel, W. Fucke, H. Wadle, 1980; *Die Bestimmung thermophysikalischer Daten flüssiger hochschmelzender Metalle mit schnellen Pulsaufheizexperimenten*, P Mannhold, Düsseldorf.
- 10. R. Hultgren, P. D. Desai, D. T. Hawkins, M. Gleiser, K. K. Kelley, and D. D. Wagman, *Selected Values of the Thermodynamic Properties of the Elements* (American Society of Metals, 1973).
- 11. A. Cezairliyan, A. P. Miiller, *Int. J. Thermophys.* **6**:191 (1985).
- 12. K. S. Sukhovei, *Soviet Phys. Solid State* **9**:2893 (1968).
- 13. Ya. A. Kraftmakher and A. G. Cherevko, High Temp.-High Press. 7:283 (1975).
- 14. A. V. Logunov and A. I. Kovalev, High Temp.-High Press. 5:625 (1973).
- 15. T. B. Massalski, P. R. Subramanian, H. Okamoto, and L. Kacprzak, *Binary Alloy Phase Diagrams*, 2nd ed., ASM International, Materials Park, OH (1990).
- 16. J. W. Dickinson, and L. S. Richardson, *Trans. ASM*, **51**: 758 (1959).
- 17. E. M. Savitskii, M. A. Tylkina, and L. L. Shishkina, *Izv. Akad. Nauk SSSR*, *Otd. Tekhn. Nauk, Met. Toplivo*, **3**: 99 (1959).
- 18. W. Obendrauf, E. Kaschnitz, G. Pottlacher, and H. Jäger, Int. J. Thermophys. 14 417 (1994).
- 19. C.Otter, G. Pottlacher and H. Jäger, Int. J. Thermophys. 17:987 (1996).
- 20. A. Cezairliyan, S. Krishnan and J. L. McClure, Int. J. Thermophys. 17:71455 (1996).
- 21. K. C. Mills, B. J. Monaghan and B. J. Keene, NPL Report CMMT(A) 53 (1997).
- 22. E. Kaschnitz, G. Pottlacher, and H. Jäger, Int. J. Thermophys. 13:699 (1992).
- 23. J. L. McClure and A. Cezairliyan, Int. J. Thermophys. 13:75 (1992).
- 24. A. Cezairliyan, J. Chem. Thermodynamics. 6:735 (1974).
- 25. A. Seifter, 1996 Diploma-Thesis, Technische Universität Graz.